AIAA-96-1381; 37th AIAA/ASME/ASCE/AHS/ASC Structures, Structural Dynamics, and Materials Conference, Salt Lake City, UT, April 15-17, 1996.

EFFECTS OF ALTERNATIVE WING STRUCTURAL CONCEPTS ON HIGH SPEED CIVIL TRANSPORT LIFE CYCLE COSTS

William J. Marx* **Dimitri N. Mavris†** **Daniel P. Schrage‡**

Aerospace Systems Design Laboratory
School of Aerospace Engineering
Georgia Institute of Technology
Atlanta, GA 30332-0150

Abstract

An integrated design and manufacturing approach allows economic decisions to be made that reflect the entire system design as a whole. In order to achieve this objective, integrated cost and engineering models were developed and utilized within a focused design perspective. A framework for the integrated product and process design of an aircraft system with a combined performance and economic perspective is described in this paper. This framework is based on the concept of *Design Justification* using a Design for Economics approach. A production cost model is developed that is sensitive to material and product/process selections for the wing structure. The use of cost/time analyses is described and applied for evaluation of process trades at the sub-component level of design. Results of an Integrated Product/Process Development (IPPD) case study are presented for potential High Speed Civil Transport (HSCT) wing structural concepts. Cost versus performance studies indicate that an aircraft with a hybrid wing structural concept, though more expensive to manufacture than some homogeneous concepts, can have lower direct operating costs due to a lower take-off gross weight and less mission fuel required.

List of Symbols

x	production unit number
γ_x	xth unit cost
Q_0	a pre-specified production quantity
v	learning curve slope
ω	weight sizing curve slope
w	material weight
w_0	a pre-specified finished-material weight
ρ_l	labor rate
$\bar{f}$	average annual percentage inflation rate
y_0	base year
y	current year
σ_m	raw material cost
ϕ_m	material buy-to-fly ratio
ψ_m	material burden rate
γ_{x_l}	xth unit labor cost
λ_{x_m}	xth unit material cost
γ_{cx_l}	cumulative labor cost through xth unit
λ_{cx_m}	cumulative material cost through xth unit
ξ_l	generalized labor theoretical first unit cost
ξ_m	generalized mat'l theoretical first unit cost
x_b	learning curve break-point unit

* Ph.D. Candidate, School of Aerospace Engineering. NASA LaRC GSRP Fellow. Student member AIAA.
email: bmarx@cad.gatech.edu
http://www.cad.gatech.edu/asdl/bill
† Manager, ASDL. Assistant Professor, Member AIAA.
‡ Co-Director, ASDL. Professor, Member AIAA.

Introduction

Product designs can be evaluated with several well known and common metrics. Aircraft take-off gross weight, component weights, wing tip deflections, and flutter boundaries are common examples of product metrics used to evaluate alternative structural design concepts. The integration of manufacturing knowledge into the design process is a technical challenge that implicitly proposes a new problem: *What metrics should be used to evaluate designs in terms of their process characteristics*? The most logical process metric is cost. The term "cost" implies many concepts, each of which may be best suited to evaluate a particular part of a production model.

Aerospace manufacturers today are searching for techniques to gain a sustainable, competitive advantage in the global marketplace. As methods are being developed for integrating design and manufacturing, the

area itself is broadening in scope. Several disciplines in both the fields of design and manufacturing separately become involved with any integration development. Many techniques and systems have been developed for providing producibility guidance to the designer,[1-6] for determining the cost implications of structural design decisions earlier in the design process,[7-9] and for design-to-cost applications.[10-14] Current efforts are focusing on making cost an independent design variable in the design and optimization process itself.[15]

The idea of designing an aircraft with substantial early regard to manufacturing cost is a relatively new concept. Most systems designs of the past have been designed with performance being the main objective function; however, this is no longer possible in today's marketplace. The emphasis on lowering all aspects of Life Cycle Costs (LCC) is leading to the development of new techniques to address LCC early in the design process. The use of cost models concurrently with design models brings with it many technical challenges, including the issues of data fidelity and the mapping between product and process design variables.

Approach

Traditional justification procedures often fail to capture the relevant information and factors necessary to justify investment in a particular technology for production. An approach developed by Noble & Tanchoco[16] proposes the consideration of the system justification concurrently with its design. With such an approach, it should possible to design a system and justify its development and implementation. The technique was originally proposed for the design of manufacturing systems, but is applied to the integrated design and manufacturing of an aircraft major component for this research.

In general, the economic justification of a design is the determination of whether a particular action or decision is justifiable based upon its economic consequences. *Design Justification* is a term used to describe a design process in which the economic ramifications of design decisions are considered concurrently with design development and are used to guide the design process to result in an economically feasible solution that meets the [mission and] performance requirements of the design.[17]

Addressing cost concurrently with the performance characteristics of the design can alleviate a common problem for economic justification. In the implementation used for this research, the mapping of system cost variables to performance design variables is not done by the cost analyst after the design is completed. Instead, the use of integrated engineering and cost models allows the cost data to be generated and analyzed as the physical system is being designed. The mapping occurs through the analysis code integration.

Typically, design economics are not evaluated until a design concept is relatively mature. At this point, most of the design's incurred costs have been fixed. The *Design Justification* process requires simultaneous performance and economic evaluations for the aircraft systems, as illustrated in Figure 1.

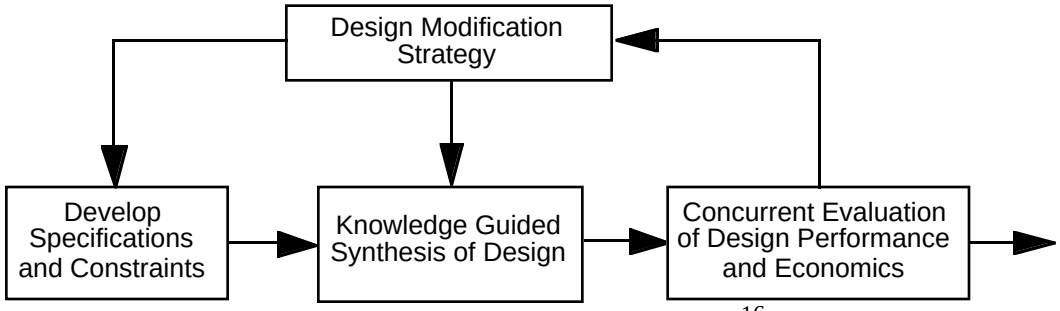

Figure 1 *Design Justification* Process[16]

Design Justification is characterized by four concepts: it is simultaneous, goal-directed, decision-maker centered, and knowledge-guided.[16] These four concepts separate the approach from the traditional, sequential approach that has been used to design most existing aerospace systems. The four elements are briefly described in the following sections. The goal-directed nature of the *Design Justification* process and its relation to Integrated Product/Process Development (IPPD) is described in more detail because of its importance for structuring the concept evaluation trade studies.

Simultaneous Design Effort

Integrated engineering and cost models are required for *Design Justification*. The simultaneous consideration of the performance (or product design) characteristics of a design and its associated cost (or

process design) characteristics allows *Design Justification* as the design matures. Detailed cost analyses conducted during the design process allow the key cost drivers to be discovered and addressed before the design matures to a point beyond which re-design costs are too expensive to be implemented.

Goal-Directed Design

A goal-directed design process is one in which the goals or objectives of the design are specified, and can be modified, by the designer and are used during the design process to direct the analysis. At phases during the design process, an analysis of the possible benefits from variables that could improve performance and economic characteristics must be conducted. The simultaneous consideration of the design's product and process design characteristics during *Design Justification* is known as IPPD. Figure 2a shows a conceptual IPPD framework for aerospace systems design.

Integrated Product and Process Development

Figure 2a illustrates the decomposition activities from conceptual design (system level) to preliminary design (component level) to the detail design (part level) and manufacturing process level in a clockwise manner on the outer circle. Continuing clockwise leads to the *recomposition* activities, from part to component to system level. The inner loops on the top portion of the figure represent integrated product/process trades at the system level. The middle loop represents the same, except for *component* level product/process trades. Similarly, the lower loop corresponds to *part* level trades for products/processes. An iteration around the long outer loop represents what has typically been done in past sequential system design; re-design was often required due to product design incompatibilities with manufacturing processes.

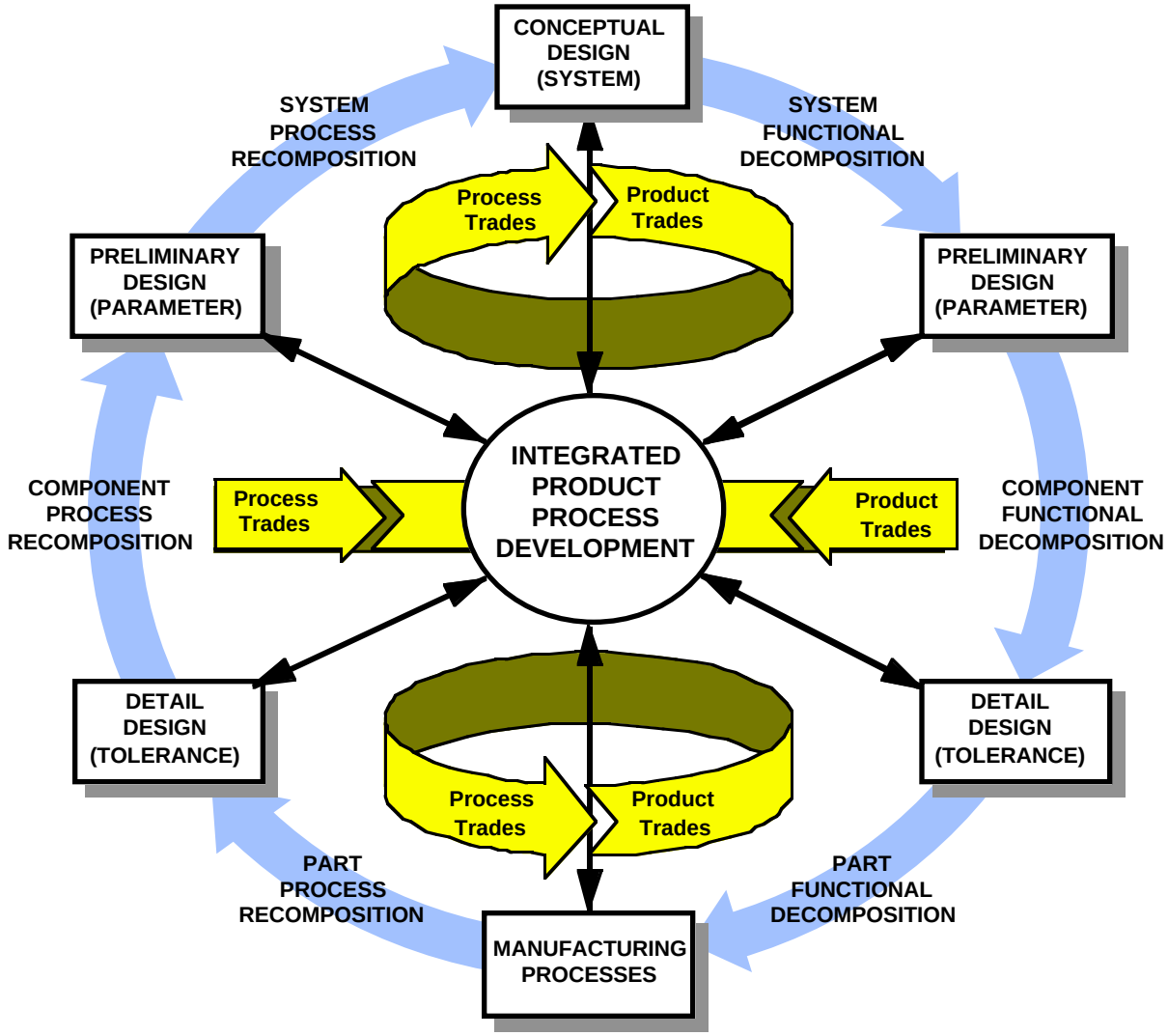

Figure 2a A Conceptual Framework for Integrated Product and Process Development

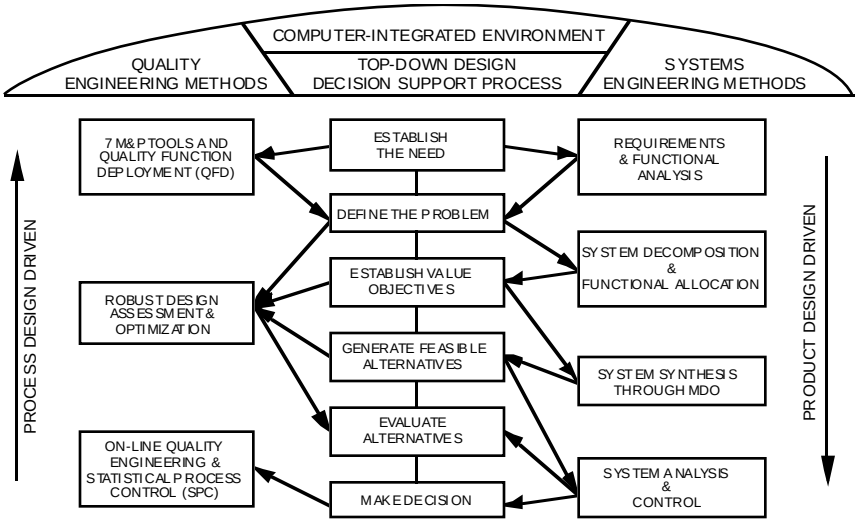

Figure 2b Interaction of the Four Key Elements to Implement IPPD

While Figure 2a represents the activities desired and information flow required for IPPD, it does not provide a methodology for integrating the tools required to implement IPPD. The practice of IPPD requires the simultaneous use of several techniques integrated in a decision support process. A generic methodology that is being used to implement IPPD at Georgia Tech is shown in Figure 2b. This methodology can be applied for the system, component, or part level trades illustrated in Figure 2a, or for an integrated combination. Illustrated in Figure 2b are the interactions of the four elements necessary for parallel product and process trades to be made at the appropriate levels of decomposition and recomposition. The four key elements are a top-down design decision support process, systems and quality engineering methods, and a computer integrated environment.

The heart of the implementation is a top-down design decision support process. Decision support is an essential element that can support a trade-off process and can be used to focus efforts on design goals. It supplies a logical, rational means for including factors that must be considered when making a decision. For the wing structural design of the HSCT, the decision support process logic starts with an identified HSCT conceptual design at the system level and an overall evaluation criterion (OEC). For the wing major component (or sub-system level), the HSCT system level requirements are deployed down to a preliminary design level. A review of candidate materials and processes, as well as panel and substructure concepts is a prerequisite for the generation of alternative wing concepts. The feasibility of the concepts is determined with a detailed structural analysis to satisfy both static and dynamic load cases. Evaluation of the alternatives is typically based only on product metrics such as the primary wing structure weight. If cost is included as a product metric, it is also weight-based. In this paper, the evaluations of the feasible concepts will also be based on time/cost process metrics such as fabrication, assembly, and material costs. With the developed integrated design system, the structural concept selection can be based upon evaluation of both the product and process metrics that characterize the concepts.

The systems engineering methods on the right side of Figure 2b are decomposition-oriented and product design driven. The flight conditions of the HSCT mission profile determine the aerodynamic and structural requirements for the wing structure. Data from a finite element structural analysis and optimization of the wing structure are used to re-size aircraft for different wing concepts and constitutes the system synthesis. System analysis is typically based on product design metrics, but, in this paper, also includes process metrics.

The quality engineering methods illustrated on the left side of Figure 2b are recomposition-oriented, statistically-based, and process design driven. The recomposition process starts at the bottom of the figure with use of quality or value engineering estimates of the manufacturing process step times to manufacture the wing structure. A process-based assessment of the design in terms of its production costs at the major component level is used in the evaluation of the feasible alternatives. For top-level IPPD studies, a Quality Function Deployment (QFD) technique is very useful to help define the design problem once the need has been established, and track and deploy the decision-making process. However, it has not been included for this IPPD trade-off process for the wing structure.

The top of Figure 2b illustrates how the three previously described elements function within a computer integrated environment. This environment allows the interactive involvement of the three elements, indicated by the arrows between elements.

The IPPD trade studies associated with the evaluation of alternative wing structural concepts required the integration of several design tools into a functional design system.

Decision-Maker Centered Design Approach

The emphasis of the *Design Justification* procedure is information processing and presentation in an appropriate manner to aid the designer. A design-process centered approach requires the analysis of a design against a set of weighted criteria, resulting in a recommended solution. A decision-maker centered approach, on the other hand, requires the data generated during the design to be received by the designer and processed with guidance. The designer can conduct sensitivity analyses to determine the advantages or disadvantages of allowing the design to progress in one direction over another.

Knowledge-Guided Design Approach

As opposed to many current systems design techniques, *Design Justification* is knowledge-guided. With a non-knowledge-guided approach (Figure 3), the conceptualization of the design is done strictly by the designer. A problem is modeled to a particular level of fidelity, then analyzed and interpreted. The designer can modify the model until it meets the design objectives.

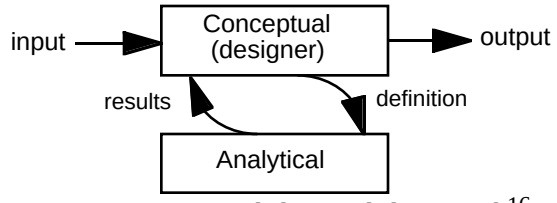

Figure 3 Non-Knowledge-Guided Approach[16]

While such a process is sufficient for many cases, design problems that require interpretation of heuristic knowledge can not be handled. The knowledge-guided design approach (Figure 4) has an additional component to handle heuristic problems: explicit knowledge. This approach allows the designer to model his system *and* guide the design process utilizing the knowledge component.

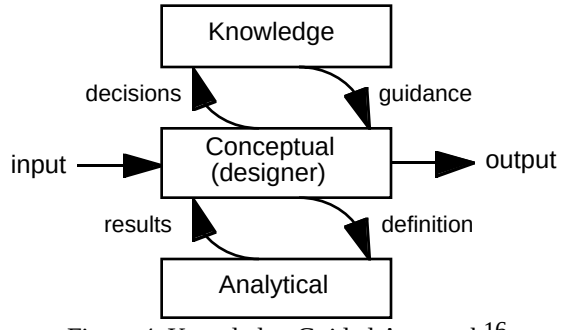

Figure 4 Knowledge-Guided Approach[16]

The knowledge component could theoretically exist in many forms; a Knowledge-Based System (KBS) was used for this project.

Implementation of *Design Justification*

The implementation of the *Design Justification* process required three areas of research and development. First, it involved the acquisition/development of a body of manufacturing knowledge. This was based on several previous supersonic transport studies,[18-28] as well as studies of candidate materials and processes to be used for the HSCT.[24,29-32] The most relevant knowledge was embodied in a Knowledge-Based System, CLIPS,[33] (C Language Integrated Production System) which was used for this research.

Second, a production cost model for the wing that captures the effects of alternative materials and manufacturing processes was developed. This also included determining the most appropriate techniques to present the product and process trade results to the designer.

Third, the process design tools were integrated with product design tools to form a functional design system (corresponding to the computer integrated environment of Figure 2a). Several pre- and post-processors and integration scripts were written to link the KBS with a top-level LCC model and an aircraft sizing code. FLOPS[34] (Flight Optimization System) was used to size the aircraft and the production cost model became a new module within ALCCA (Aircraft Life Cycle Cost Analysis).[35] The integration enables designers to quantify where and how the processing costs produce significant effects and propagate through the aircraft's life cycle. The integration of the sizing code into the evaluation framework and the automated data mapping and passing alleviates distortions in data due to communication of results between analysis processes.

Details of all three of these components are beyond the scope of this paper. The KBS is described by Marx *et al*[36] and the multi-level LCC model developed with ALCCA is discussed in Marx *et al*.[37] Details of the wing production cost model are presented in the following section.

Wing Production Cost Model

It was necessary to develop and implement a new production cost module for the LCC code. The form of the previous weight-based wing cost equation in ALCCA was:

$$Cost_{wing} = a \cdot cf \cdot \left(Weight_{wing} \right)^{b \cdot ef} \quad (1)$$

where a and b are based on a historical database of aluminum aircraft (wings) and cf and ef are complexity factors that can be used to adjust the costs for titanium or composite wings.

For a complex, integrated structure like the HSCT wing, such a model is not sufficient. Cost Estimating Relationships (CERs) developed for estimating wing costs are usually based on a historical database of existing wings. Virtually all of those wings would have been manufactured from aluminum. In addition, most of the wings undoubtedly have a much higher aspect ratio than the HSCT wing. Hence, application of the existing wing CER in ALCCA was not a feasible option for the HSCT wing.

Since lower weights do not always signify reduced costs, a model based only on component weights will not show the correct trends for many new advanced materials and manufacturing processes. Several examples of this trend exist, including the use of thermoplastics versus thermosets. Thermoplastic materials are often selected by the product design teams, but are replaced with thermosets once more realistic cost/time manufacturing information is obtained, especially for large thermoplastic components.

The new model includes both labor and material costs for the wing. Calculation of the production costs both in terms of hours and dollars allows sensitivity studies to be conducted based not only on component weights versus costs, but also production times, labor rates, raw material costs, buy-to-fly ratios, and alternate processing methods versus many cost and time elements.

Using the typical exponential function form of the learning curve, the x^{th} unit cost, γ_x, as a function of a known $Q_0{}^{th}$ unit cost, γ_{Q_0}, and learning curve slope can be written as:

$$\gamma_x = \gamma_{Q_0}(Q_0)^{-\beta} x^{\beta} \tag{2}$$

where:

$$\beta = \frac{\ln(\nu)}{\ln(2)} \tag{3}$$

and ν is the decimal value of the slope of the given learning curve. If γ_x represents the x^{th} unit cost for a pre-specified finished material weight, equation (2) can be modified as:

$$\gamma_x = \gamma_{Q_0}\left(\frac{1}{Q_0}\right)^{\beta}\left(\frac{w}{w_0}\right)^{\eta} x^{\beta} \tag{4}$$

where:

$$\eta = \frac{\ln(\omega)}{\ln(2)} \tag{5}$$

with ω as the decimal value of the slope of the weight sizing curve, w is the material weight, and w_0 is the pre-specified finished material weight upon which the unit costs are based.

Assume equation (4) represents costs in terms of direct labor hours. It can be transformed to dollar costs by multiplying by a labor rate, ρ_l. Inflation effects must be accounted for to scale CERs developed for a specific year's dollars. Recognizing that inflation has a compounding effect similar to interest, equation (4) can now be written as:

$$\gamma_{xl} = \gamma_{Q_0}\left(\frac{1}{Q_0}\right)^{\beta}\left(\frac{w}{w_0}\right)^{\eta} \rho_l (1+\bar{f})^{(y-y_0)} x^{\beta} \tag{6}$$

where $\bar{f}$ represents the *average* annual percentage inflation rate over the period of years from y_0 to y.

An equation for unit x material costs can be developed similarly:

$$\lambda_{xm} = w\sigma_m\phi_m\psi_m\left(\frac{1}{Q_0}\right)^{\beta}\left(\frac{w}{w_0}\right)^{\eta} (1+\bar{f})^{(y-y_0)} x^{\beta} \tag{7}$$

where w is the material weight, σ_m is the raw material cost, ϕ_m is the material buy-to-fly ratio (corresponding to a scrap rate), and ψ_m is the material burden rate.

The cumulative labor and unit costs are found by multiplying equations (6) and (7) by x, the cumulative number of units produced to yield:

$$\gamma_{cxl} = \gamma_{Q_0}\left(\frac{1}{Q_0}\right)^{\beta}\left(\frac{w}{w_0}\right)^{\eta} \rho_l (1+\bar{f})^{(y-y_0)} x^{\beta+1} \tag{8}$$

$$\lambda_{cxm} = w\sigma_m\phi_m\psi_m\left(\frac{1}{Q_0}\right)^{\beta}\left(\frac{w}{w_0}\right)^{\eta} (1+\bar{f})^{(y-y_0)} x^{\beta+1} \tag{9}$$

For simplification purposes, now let ξ_l and ξ_m represent generalized labor and material Theoretical First Unit Costs (TFUCs), respectively.

$$\xi_l = \gamma_{Q_0}\left(\frac{1}{Q_0}\right)^{\beta}\left(\frac{w}{w_0}\right)^{\eta} \rho_l (1+\bar{f})^{(y-y_0)} \tag{10}$$

$$\xi_m = w\sigma_m\phi_m\psi_m\left(\frac{1}{Q_0}\right)^{\beta}\left(\frac{w}{w_0}\right)^{\eta} \left(1+\bar{f}\right)^{(y-y_0)} \tag{11}$$

Rewriting equations (6) and (7) with ξ_l and ξ_m gives

$$\gamma_{xl} = \xi_l x^{\beta} \tag{12}$$

$$\lambda_{xm} = \xi_m x^{\beta} \tag{13}$$

which now look like the more familiar form of the learning curve equation.

This production cost model formulation so far implicitly implies a single learning curve function. However, production functions are not always best represented by a single learning curve. The following formulation further develops the production cost labor equations for a double learning curve.

A double learning curve formulation implies two distinct learning curve slopes, ν_1 and ν_2. This leads to two values for β; let

$$\beta_1 = \frac{\ln(\nu_1)}{\ln(2)} \qquad \beta_2 = \frac{\ln(\nu_2)}{\ln(2)} \tag{14}$$

For a learning curve breakpoint, x_b, equation (12) is now written as:

$$\gamma_{xl} = \xi_l x^{\beta_1} \qquad x \le x_b \tag{15}$$

$$\gamma_{xl} = \xi_l (x_b)^{\beta_1} \left(\frac{x}{x_b} \right)^{\beta_2} \qquad x \geq x_b \tag{16}$$

Since the decrease in hours or costs due to a cumulative doubling in production is now following the second learning curve slope, ν_2, with respect to a new first unit point, namely x_b, equation (16) must include the ratio $\left(\frac{x}{x_b} \right)$ in order to have the doubling occur with respect to the cumulative number produced *after* x_b. Equation (16) can be simplified to:

$$\gamma_{xl} = \xi_l (x_b)^{\beta_1 - \beta_2} x^{\beta_2} \qquad x \geq x_b \tag{17}$$

Using a basic property of the natural log function, equation (18) can be written:

$$\gamma_{xl} = \xi_l \left(e^{\ln(x_b)} \right)^{\beta_1 - \beta_2} x^{\beta_2} \qquad x \geq x_b \tag{18}$$

or:

$$\gamma_{xl} = \xi_l e^{\delta} x^{\beta_2} \qquad x \geq x_b \tag{19}$$

where:

$$\delta = (\beta_1 - \beta_2) \ln(x_b) \tag{20}$$

Equation (19) now represents the corrected form of the equation for the cumulative labor cost after the production breakpoint, x_b, following the second learning curve slope, ν_2. To summarize, the labor cost equations with a production breakpoint are:

$$\gamma_{xl} = \xi_l x^{\beta_1} \qquad x \leq x_b \tag{21}$$

$$\gamma_{xl} = \xi_l e^{\delta} x^{\beta_2} \qquad x \geq x_b \tag{22}$$

and the cumulative labor costs are now:

$$\gamma_{cxl} = \xi_l x^{\beta_1 + 1} \qquad x \leq x_b \tag{23}$$

$$\gamma_{cxl} = \xi_l e^{\delta} x^{\beta_2 + 1} \qquad x \geq x_b \tag{24}$$

Equation (13), the material costs, can also be similarly modified for a double learning curve.

The implementation of this model required actual data for several of the variables in the equations. A study by Resetar *et al*[38] provided data for recurring manufacturing costs, tooling costs, raw material costs, buy-to-fly ratios, and labor rates for a variety of advanced airframe materials.

Cost/Time Analysis

As stated previously, the emphasis of the *Design Justification* process is information processing and *presentation in an appropriate manner to aid the designer*. With the wing production cost model as formulated above, the designer can determine the manufacturing costs, tooling costs, inspection costs, and material costs for the wing structure. By perturbing certain variables, an almost endless combination of sensitivity analyses can be conducted. The analysis and interpretation of the cost and time data output from the wing production cost model is a complex task in itself. The Design Guide for Producibility[39] suggests the use of cost/time analysis plots for interpreting production cost estimates.

Figure 5 shows a generic plot of a cost/time analysis for a theoretical production operation. The x-axis is the unit cost while the y-axis represents the cumulative production time. The steps that comprise a process model for a manufacturing function are time-based, and translate to respective costs. For a particular production quantity, the sum of the steps traces a path on the plot, shown with the dashed line, to the end point, represented with a small circle.

Learning curve effects will be reflected in the cost/time analysis plot. The farthest point on the lower right of the cost/time curve represents the TFUC. Intuitively, the TFUC has the highest cost per unit. As the production quantity increases and the learning curve effects are realized, the cost per unit decreases along the cost/time curve. Different process steps, learning curves, labor rates, and production quantities will produce noticeable effects on the cost/time curves. Families of cost/time curves can be generated to show the effects of process alternatives at any level of the production, to determine the most significant cost drivers so that efforts can be focused to lower production costs, and to serve as process constraint curves for product/process design trades.

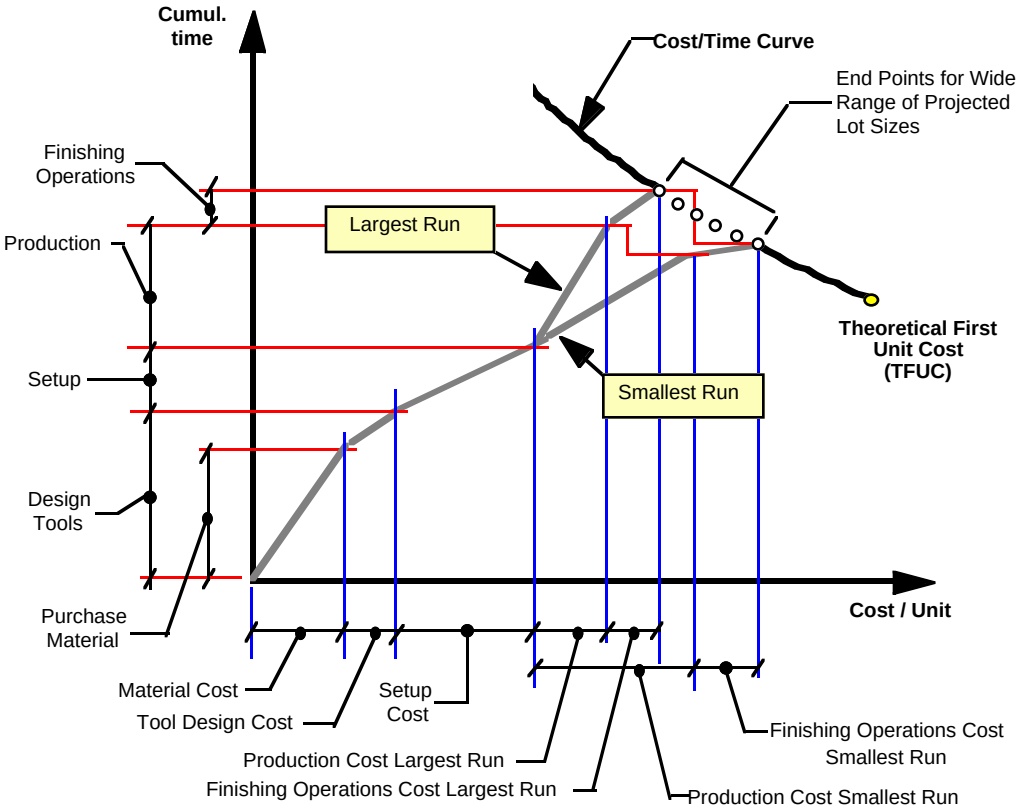

Figure 5 Cost/Time Analysis for Theoretical Production[39]

System and Model Verification

The implementation is verified in this section before proceeding to the product/process trades associated with integrating design and manufacturing for a modern High Speed Civil Transport (HSCT). Limited data exists from previous industry and NASA HSCT studies. Economic data for model verification is particularly scarce since most companies consider their data related to production costs highly competition sensitive. This section presents a summary of the detailed system and model verification that was completed before the HSCT case study was started.

Summary of the Lockheed SST Evaluation Process

Analytical design studies were performed by the Lockheed-California Company in the 1970s to assess the relative merits of several structural arrangements, concepts, and materials applicable to an arrow-wing Supersonic Transport (SST) configuration, shown in Figure 6. The Lockheed SST concept carried 234 passengers, had a cruise Mach of 2.7, and a baseline wing area of 10,900 square feet. The SST studies[18-22] resulted in a large amount of published data. Much information exists in the reports from the various disciplines, including performance and weights. The published production cost data, though not comprehensive, is believed to be the most complete non-proprietary set of data that could be found for verification of the production and economic models.

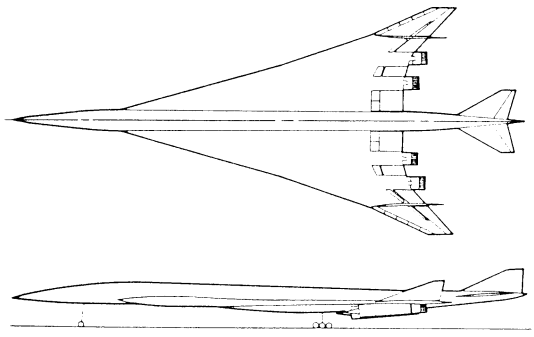

Figure 6 Lockheed SST Arrow-Wing Concept[21]

An initial structural analysis screening was conducted by Lockheed on many potential wing structural concepts. These included the chordwise stiffened, spanwise stiffened, and biaxially stiffened (monocoque) concepts shown in Figures 7-10. Unit weights were calculated for point design regions on the wing for each concept. There were three point design

regions: the forward strake area, the inboard wing box, and the outboard wing box. By interpolating from the analysis point design regions, the unit weights derived during the initial screening were applied over all design regions to derive the total box structural weight for each prospective concept. Results of Lockheed's initial structural concept screening led to a more detailed analysis of five structural concepts: a chordwise-stiffened, convex beaded concept; a spanwise hat-stiffened concept; a mechanically fastened, biaxially-stiffened, honeycomb concept; a welded, biaxially-stiffened, honeycomb concept; and a boron-polyimide reinforced chordwise-stiffened concept.

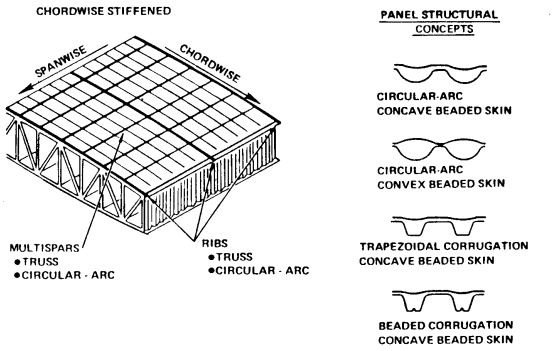

Figure 7 Chordwise Stiffened SST Wing Concepts[21]

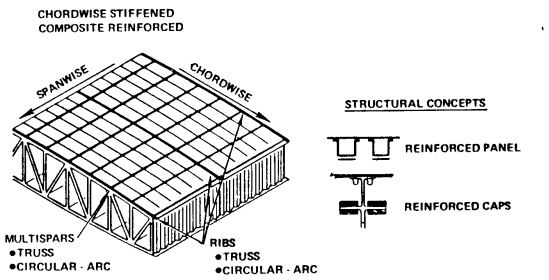

Figure 8 Composite Reinforced SST Wing Concepts[21]

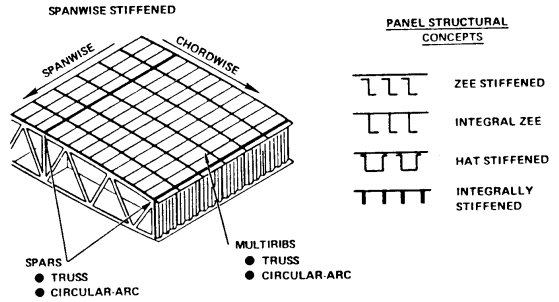

Figure 9 Spanwise Stiffened SST Wing Concepts[21]

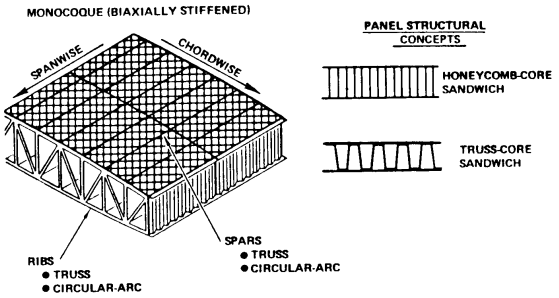

Figure 10 Monocoque SST Wing Concepts[21]

The wing weights were categorized as primary structure (variable weight) or secondary structure (fixed weight). The primary structure consists of that structure which carries the primary load and is influenced by the structural concept being evaluated, or in other words, the upper and lower skin panels and stiffeners, spars, and ribs. The secondary structure is that structure which is not as directly affected by the structural concept choice (such as flaps and ailerons).

The structural mass of each aircraft configuration was estimated first based on the premise of a fixed vehicle size and taxi weight. This permits the determination of the allowable fuel for the aircraft, which ultimately yields the range capability. The costs were subsequently determined for each configuration. The disadvantage to using this approach was that, though the relative flyaway costs could be compared, the concepts could not be compared on an equivalent performance basis, since their respective mission capabilities (i.e., range, in this case) were different. This led to a re-sizing of all configurations for a constant payload/range requirement. The payload was held constant, the range was constrained, and the gross weight of the aircraft was allowed to vary to meet the desired range goal. Following the re-sizing, the concept evaluation could be performed on a minimum-total-system-cost (with regards to operating cost variations) for concepts that had the same mission capability.

A relatively detailed description of the production hours required for producing the wing structural concepts was published.[19] The estimations included material dollars and fabrication (including subassembly) and assembly (including tank seal) hours. However, the "bottom line" of Lockheed's production cost analyses was a "value-per-pound" factor for each concept that was subsequently used for the economic evaluations. With the use of these "value-per-pound" factors, the economic subroutines within ASSET (Advanced System Synthesis and Evaluation Technique, a Lockheed sizing code from the 1970s) were used to estimate the flyaway

costs for five aircraft, based on a total production of 300 units.

Weight-Based Cost Model Limitation

To prove the limitations of current weight-based cost models concerning process variations, the results of Lockheed's SST sizing analysis were used in a weight-(only)-based LCC analysis (i.e., ALCCA, without the production data from CLIPS). The calculated system costs do not reflect the process-dependent material, fabrication, tooling, and assembly costs. Figure 11 shows the incorrect weight-based system flyaway costs for the constant-payload aircraft generated in this fashion.

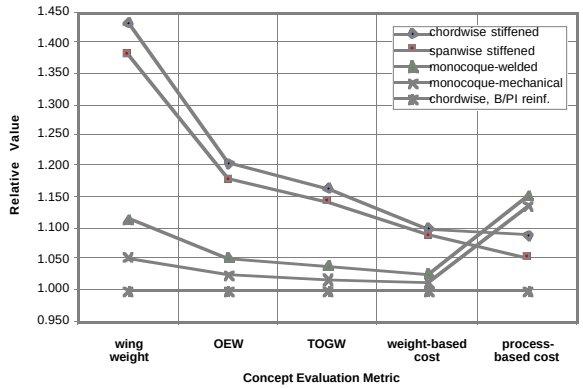

Figure 11 Weight-Based LCC Model Limitation

The highest *weight* concept, the chordwise-stiffened configuration, is also the highest *cost* concept using a weight-based LCC model (the fourth column in Figure 11), which is incorrect in this case. The two monocoque (biaxially stiffened) concepts are actually the most expensive concepts (the fifth column in Figure 11), even though their wing weights, OEWs, and TOGWs are substantially lower than those of the chordwise and spanwise stiffened concepts.

Hence, the product decomposition and process recomposition (Figures 2a and 2b) required for IPPD must occur if the LCC estimates are to reflect process variations. This must include a preliminary structural analysis to generate data beyond the major component weights. If the LCC analyses are based on only component weights, process variations will have little effect on cost.

Production Cost Model Verification

All costs calculations in ALCCA for this verification were based on a total production of 300 units. The costs for the SSTs were originally calculated using 1973 dollars; those calculated in ALCCA are in 1992 dollars. The results can be presented on an equivalent economic basis using either of two simple methods. First, the flyaway costs estimated in 1973 dollars could be inflated to 1992 dollars, or vice versa. Second, the relative flyaway costs could be presented. Since the relative costs (both flyaway and operating), as functions of wing structural concepts, will be more useful for eventual HSCT cost/benefit studies, the relative SST costs will be discussed in the following sections for both the constant TOGW and constant payload-range SSTs.

Constant TOGW SST

The system costs, normalized with respect to the composite-reinforced concept, as predicted with the integrated system developed for this research, are given in the Table 1 for the constant 750,000 pound TOGW aircraft. The relative differences of the predicted values, with respect to Lockheed's original estimates are also included for comparative purposes.

All of the predicted trends are correct with respect to the composite reinforced concept. The wing concepts with the highest areal weights (the chordwise and spanwise stiffened all titanium concepts) display flyaway costs lower than the composite reinforced concept. However their range capability was far below that of the boron/polyimide concept. The biaxially stiffened concepts had higher flyaway costs than the composite reinforced concept, even though their range

Table 1 SST Concept Relative System Costs for Constant TOGW

structural arrangement	units	chordwise (mechanical)	spanwise (mechanical)	monocoque (mechanical)	monocoque (welded)	chordwise (B/PI reinf)
Constant TOGW (Lockheed):						
flyaway cost	$1973M	0.966	0.951	1.119	1.117	1.000
DOC	c/sm	1.010	1.000	1.057	1.063	1.000
IOC	c/sm	1.044	1.033	1.011	1.011	1.000
Constant TOGW (ALCCA):						
flyaway cost	$1992M	0.977	0.971	1.095	1.020	1.000
DOC	c/sm	1.025	1.023	1.041	1.018	1.000
IOC	c/sm	1.027	1.024	1.014	1.014	1.000
Relative differences:						
flyaway cost		1.12%	2.11%	-2.09%	-8.73%	0.00%
DOC		1.42%	2.31%	-1.52%	-4.17%	0.00%
IOC		-1.66%	-0.93%	0.24%	0.24%	0.00%

capabilities were less than that of the composite concept. This is due to the fact that significantly more production hours were required to fabricate the sandwich panels than the more conventionally stiffened panels. The composite reinforced concept was considered a higher technology concept than the biaxially stiffened concepts, but had a lower wing areal weight and, thus, a lower TOGW, tended to offset the costs incurred through an increase in technology level.

Though the flyaway cost of the welded monocoque structure was correctly estimated to be greater than that of the composite reinforced concept, the magnitude of the difference was not as great as that predicted with ASSET. This discrepancy, which is only evident for this particular concept, can be explained as follows. The "value-per-pound" factors used with ASSET in the Lockheed-California studies accounted for material cost, fabrication and assembly hours, and tooling hours. For the welded, biaxially stiffened concept, the material and tooling "value-per-pound" factors were not significantly different. However, their predicted production hours required for the mechanically fastened, monocoque concept were three times greater than what was predicted for the welded, monocoque concept. This does not correspond to the published values for the flyaway costs of these concepts being almost equal. ALCCA's predictions for the flyaway costs for the biaxially stiffened concepts were consistent with the number of hours required to produce the concepts, an advantage to using a model based on time (hours), as opposed to applying factors to weight-based algorithms only.

The operating cost calculations correlate with ASSET's predictions as well. A minor difficulty in verifying the models was the realization that the published operating costs for the constant TOGW aircraft were for operation at the calculated design range. This again, is another difficulty in attempting to do a consistent economic concept evaluation with concepts that do not have the same mission capability. However, once the appropriate stage lengths were used in the DOC and IOC calculations, the ALCCA-predicted values correlated well with the ASSET values, again with the exception of the welded monocoque concept. Both of the predicted values for the welded monocoque concept's DOC are consistent with the estimated values of the flyaway costs. Or, in other words, an increase (or decrease) in flyaway cost (or acquisition price for the airlines) should lead to an increase (or decrease) in the DOC for the aircraft because of the cost of ownership portion of the DOC (depreciation, interest, and insurance costs). Lockheed's predicted value for the DOC is consistent with their predicted value for the flyaway cost for the welded concept; ALCCA's is consistent as well.

Constant Payload-Range SST

The relative system costs, as calculated with the integrated system, are given in Table 2 for the constant payload-range aircraft. These aircraft were all required to meet the 4,200 nmi range requirement. Though the TOGWs were significantly different, the aircraft can better be compared on an equivalent economic basis since they all have the same mission capability. Again, the original estimates by Lockheed are included for comparison.

Table 2 SST Concept Relative System Costs for Constant Payload-Range

structural arrangement	units	chordwise (mechanical)	spanwise (mechanical)	monocoque (mechanical)	monocoque (welded)	chordwise (B/PI reinf)
Constant Payload-Range (Lockheed):						
flyaway cost	$1973M	1.089	1.054	1.135	1.155	1.000
DOC	c/sm	1.109	1.083	1.067	1.093	1.000
IOC	c/sm	1.044	1.044	1.011	1.011	1.000
Constant Payload-Range (ALCCA):						
flyaway cost	$1992M	1.093	1.072	1.082	1.010	1.000
DOC	c/sm	1.115	1.097	1.048	1.033	1.000
IOC	c/sm	1.034	1.030	1.010	1.007	1.000
Relative differences:						
flyaway cost		0.38%	1.72%	-4.69%	-12.55%	0.00%
DOC		0.57%	1.31%	-1.84%	-5.52%	0.00%
IOC		-1.02%	-1.34%	-0.10%	-0.43%	0.00%

The flyaway costs for the constant payload-range concepts again all exhibit the same trends as those predicted by Lockheed. In this case, the composite-reinforced concept is simply the lowest cost alternative. Though the non-composite reinforced, chordwise stiffened concept and the spanwise, hat-stiffened concept had the lowest flyaway costs in the case for constant TOGW, their flyaway costs are now higher than that of the composite-reinforced concept. This is due to the fact that, during the re-sizing for constant payload-range, their OWEs and TOGWs increased significantly, resulting in an increase in their flyaway costs. The monocoque welded concept exhibited the same

characteristics in this case as it did when constrained to a maximum TOGW of 750,000 lbs.

The operating costs were easier to verify for this constant payload-range case. All stage lengths (4,200 nmi) were equal. The ALCCA-predicted values were consistent with those predicted by ASSET.

The results presented in this section display excellent correlation with the most comprehensive set of non-proprietary data available for SST model and system verification. All of the relevant trades, for both performance and economics, have been verified. With the use of a powerful LCC code like ALCCA, integrated with a production cost KBS and a sizing code, it is possible to show the effects of alternative structural concepts in cost/benefit studies. In addition, with automated data passing, file preparation, and pre- and post-processing utilities, it is now possible to show the effects of alternative concepts or process implications on several constituents of the Life Cycle Cost at the desired level of fidelity. This will be demonstrated for the HSCT wing structural concept.

The use of a Knowledge-Based System "in the loop" with an integrated sizing code and multi-level Life Cycle Cost analysis model appears to be an excellent way to determine both the performance and economic consequences of conceptual and preliminary structural design decisions.

Hence, the integration scheme and system level wing areal weight modeling assumptions are valid for showing product/process trades for wing production costs. The source of the production data for this verification exercise was the SST studies. However, the advanced materials and processes that are projected for HSCT airframe production required a new set of production cost data. Details of the IPPD trade study conducted for the HSCT wing structure are presented in the next section.

HSCT Concept Description

The HSCT was chosen as the case study aircraft for this research for several reasons. It is currently under study by several of the U.S. aerospace industry prime and sub-contractors, as well as NASA and many universities. The technological challenges associated with this aircraft provide many topics for both industrial and academic research.

The modern HSCT concept is a 300-passenger aircraft with a design range of 5,000 nautical miles. Its cruise speed is currently set at Mach 2.4. Weight estimates range from an optimistic 750,000 pounds to over 900,000 pounds, depending on the specific configuration. The structural design life of the aircraft is targeted at 20,000 flight cycles and 60,000 flight hours. Take-off and landing field lengths are specified to be no longer than 11,000 feet.

The HSCT was modeled in FLOPS with relevant geometry, mission parameters, aerodynamic data, and propulsion data. The baseline HSCT modeled in FLOPS had the characteristics defined in Table 3.

Table 3 HSCT Configuration Description

Range	5,000 nmi
TOGW	825,000 lbs
Number of passengers	300
Cruise ceiling	70,000 ft
Approach speed	155 kts.
Fuselage length	330 ft.
Wing area	9,000 ft^2
Wing span	130 ft
Horizontal tail area	1,000 ft^2
Vertical tail area	600 ft^2
Horizontal tail sweep angle	35˚
Vertical tail sweep angle	41˚

Off-the-shelf aerodynamic design codes[40-46] were used to generate the user-defined induced drag coefficients for FLOPS. The optimum twist and camber distribution for the wing and the area-ruled fuselage were used in generating the drag polars that were input into FLOPS. A fixed cycle for a mixed-flow turbofan engine was selected from the FLOPS-supplied engine cycles.

The mission used for sizing the aircraft in FLOPS was a nominal 85% supersonic and 15% subsonic (by distance) mission. A plot of a representative split sub/supersonic mission profile generated by FLOPS is shown in Figure 12. As illustrated in Figure 12, both the subsonic and supersonic cruise segments were flown at a fixed Mach number, with the optimum altitude for specific range calculated by FLOPS.

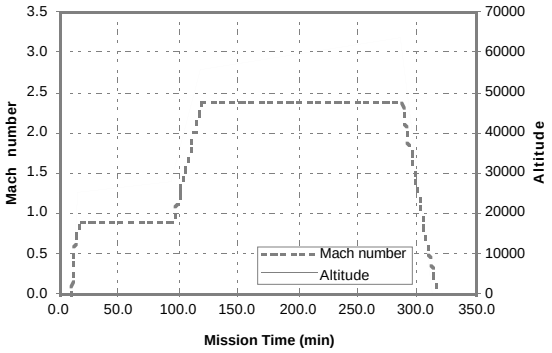

Figure 12 Mission Profile

Wing Region Descriptions

The wing is divided into three main design regions: the forward strake, the inboard (or main) wing box, and the wing tip box. Figure 13 shows a CATIA solid model of the baseline HSCT aircraft that illustrates the

three design regions of the baseline HSCT concept evaluated in this paper.

Also illustrated on the starboard side of the aircraft is the optimum twist and camber distribution of the aerodynamic grid generated for this HSCT wing planform (with the z-ordinates scaled by a magnitude of 4). The area-ruled fuselage is also clearly visible from this perspective.

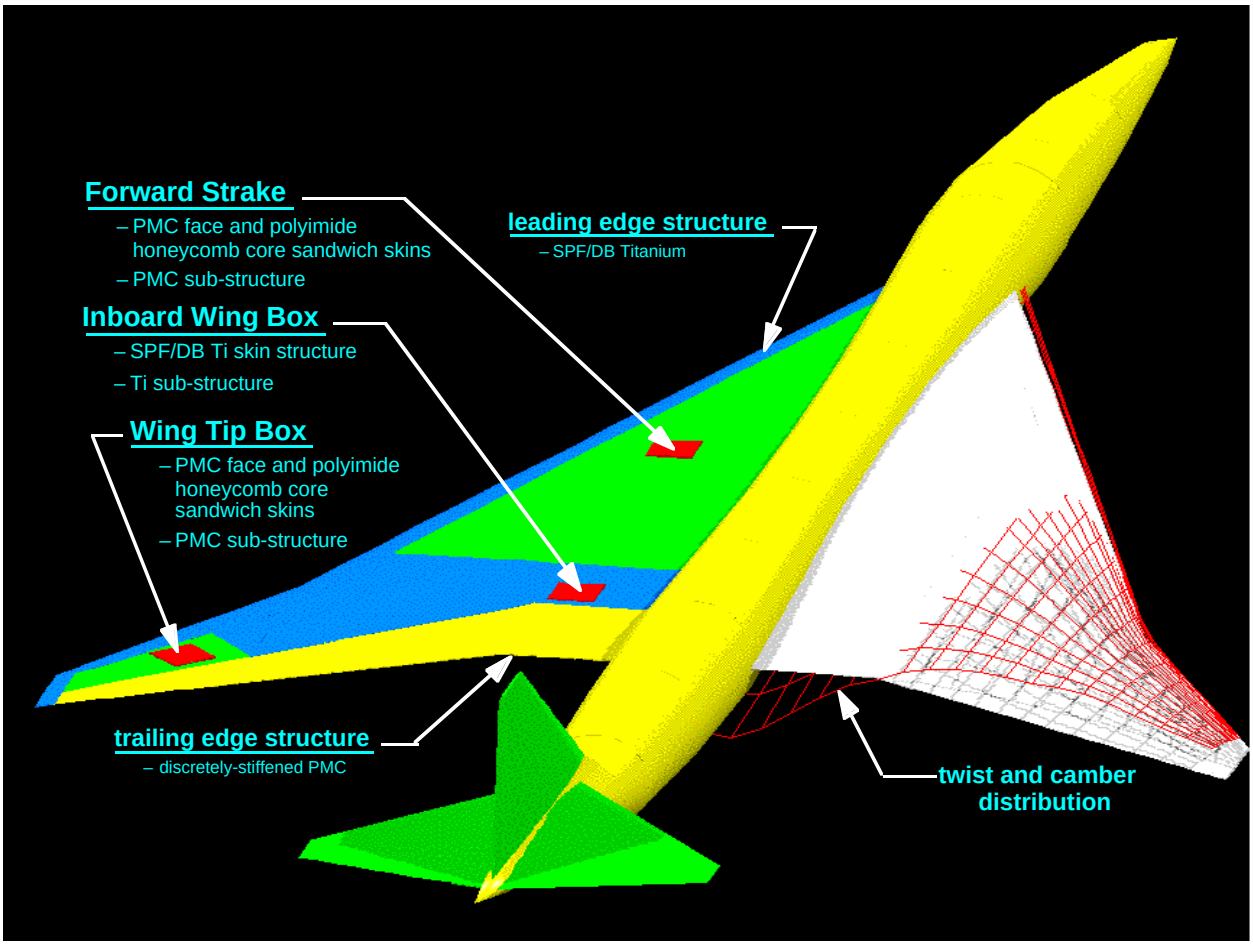

Figure 13 CATIA Solid Model Showing the Baseline Hybrid HSCT Wing Structural Concept

The baseline wing concept is representative of current concepts under study by industry. Composite honeycomb skin panels and Superplastically Formed / Diffusion Bonded (SPF/DB) titanium skin panels are viable candidates for HSCT wing structure.[2 4] Academically, a hybrid concept provides a good baseline for IPPD trade studies. Three potential HSCT wing structural concepts are evaluated in this paper using the approach and computer implementation described previously. These substantially different concepts were chosen to show a variety of trends in cost and performance.

Concept one has SPF/DB titanium skin panels and titanium substructure in all three wing design regions.[4 7] Concept two has Z-stiffened PMC skin panels and PMC substructure in all wing regions.[4 7] Concept three has the baseline hybrid wing structure[2 4] illustrated in Figure 13. While the structural product and process characteristics of the concepts were different, the planform shape and size remained constant.

In order to conduct IPPD trades, the product and process characteristics of the individual design regions were identified. The product characteristics are similar for all three concepts, but the processing characteristics are quite different. Table 4 shows the product and process characteristics for the *baseline* structural concept (concept three, the hybrid structure).

Table 4 Wing Region Product and Process Characteristics

Wing Region	Product Characteristics	Process Characteristics
Forward Strake	The forward strake region experiences light or moderate biaxial loads with respect to wing bending. Much of the forward strake is designed to meet minimum gage requirements.	The loft-to-loft distance is large in this section; access for automation is possible up to a depth of about 24" (the length of a human arm). As opposed to the conventional birdcage assembly approach, in which the internal structure is assembled first and then the skin panels are subsequently attached, this section of the wing will be assembled in reverse order. First the lower skin will be placed in its respective tool, the spar caps will then be (automatically) fastened to it. The spar webs will be fastened next, followed by the top spar caps. The upper panel, which is tool coordinated, is then placed and fastened. With this sequence of assembly steps, the *substructure* will be floated, as opposed to the wing panels being floated. The loft dimensions are very critical on this type of a wing. Therefore, the tools will be made for the skin panels to achieve the necessary tolerances. At depths of more than 24" from the skin panel, assembly will be manual (which increases the fastening cycle time). It is assumed that the spar caps and spar webs were cocured, requiring no additional stitching.
Main Wing Box	The major load path of the wing is in the inboard wing box. This section experiences high spanwise load intensities due to wing bending, and variable chordwise load intensities due to bending and torsional effects. This section has the highest average areal weights. The engine pylons are attached to the rear spar of this section. The inboard flap and spoiler will also be attached to the rear spar of this section.	A four-sheet SPF/DB titanium skin panel is used in this highly loaded section of the wing. The substructure is also all titanium, with extruded spar caps and sheet metal webs. The two inner sheets are first intermittently roll-seam welded with a cross pattern while the two outer sheets are periphery welded. The four sheets are heated to the processing temperature, and put in the SPF/DB press. Gas is injected to inflate/form the sheets; the temperature is held for diffusion bonding, followed by a cooling and unloading period. Then the panel is trimmed. No jig is needed for this procedure, since there are no stringers. The panels are integrally stiffened, hence there is a reduced fastener count. There is also no spring-back of the structure. A disadvantage in using this process is the high tooling cost for the individual dies.
Wing Tip Box	The wing tip box is the most stiffness-critical design region of the wing. This section experiences high load intensities, and is driven by stiffness constraints to prevent flutter and to ensure aileron control effectiveness. An outboard flap and spoiler, flaperon, and aileron will be attached to the rear spar of the wing top box.	A conventional assembly approach will be used for this section of the wing. The substructure will be assembled first, followed by the skin panels. One of the panels will be put on first, then drilled and removed. The other skin will be placed on the substructure and fully fastened. The first skin panel will then be tacked in place and mechanically fastened. Blind fasteners will be used on parts of the wing tip structure since the tip is relatively thin (approximately 6" loft-to-loft distance).

Relative Concept Costs

A recent study from McDonnell Douglas provided the relative data given in Table 5.[48] The objective of the study was to determine the effects of alternative structural concepts on the manufacturing (fabrication and assembly labor) hours and tooling costs for each of three design regions of the wing. The process characteristics given in Table 4 were used to generate the relative numbers given in Table 5. The causes of the high and low numbers due to the specific process characteristics of the design region and/or the structural concept are listed below the table.

Table 5 Relative Concept Costs[48]

Design Region	Aluminum Z	Titanium SPF/DB	Titanium H/C	PMC H/C	PMC Z
Forward Strake				baseline	
fabrication labor hours	1.0	0.67[h]	0.81	0.97	1.13[b]
fabrication tooling cost	1.0	1.22[d]	0.30[f]	0.36[g]	0.34[c]
assembly labor hours	1.0	0.86	0.86	0.86	1.00
assembly tooling cost	1.0	0.95	0.95	0.95	0.97
Tip Box				baseline	
fabrication labor hours	1.0	0.65[h]	0.87	1.13	1.46[b]
fabrication tooling cost	1.0	1.80[d]	0.53[f]	0.61[g]	0.61[c]
assembly labor hours	1.0	0.95	0.95	0.95	1.07
assembly tooling cost	1.0	0.92	0.92	0.92	0.94
Inboard Wing Box		baseline			
fabrication labor hours	1.0	0.77[h]	0.86	0.94	1.15[b]
fabrication tooling cost	1.0	0.98[e]	0.33[f]	0.35[g]	0.38[c]
assembly labor hours	1.0	1.24[a]	1.24[a]	1.24[a]	1.32[a]
assembly tooling cost	1.0	0.95	0.95	0.95	0.97

[a] relatively high number of fasteners needed
[b] includes stitching zee's onto the panel
[c] stitched/RFI is a low-cost tooling approach
[d] high cost of tooling (die) for the SPF/DB panels
[e] the die/jig cost is nearly that of aluminum, due to high compound curvature in this region
[f] no stretch form of skin required
[g] one-sided tooling
[h] not a time-intensive process step

Concept 1 is represented by the Titanium SPF/DB column in the table. Concept 2 data is the PMC Z column in the table. The baseline hybrid concept data is marked. The knowledge contained in Tables 4 and 5 was embodied in the rule bases in CLIPS. It was used to adjust the production cost estimates for the specific materials and processes used to manufacture the structure in each section of the wing. This way, the cost estimates generated are representative of the actual production processes and materials used to manufacture the wing structure.

Results

The results presented in this section are based on several assumptions:

1. The process-dependent parameters in the model are for the wing only.
2. The manufacturer's module in the LCC code is not a factory simulation model, but a model of the production of a single aircraft. The delivery schedule is assumed to be equivalent to the production schedule, and the order schedule proceeds the delivery schedule by the number of months in the RDT&E phase.
3. Distribution of the RDT&E costs, the manufacturing and sustaining costs, and revenue (income) are as outlined by Marx *et al.*[37]
4. All estimates are based on a production of 600 units, unless indicated otherwise.
5. The airline module in ALCCA provides an analysis of the costs and revenues an airline will experience in purchasing and operating one aircraft. Schedules for financing, depreciation, interest, tax, and cash flow are also found in Marx *et al.*[37]
6. Fuel costs were assumed to be $0.61 per gallon. The economic mission was 3,800 nmi and aircraft utilization was 5,000 hours per year. The load factor was 0.65. The aircraft was assumed to be financed at an interest rate of 8% over a 20 year economic lifetime for the aircraft.
7. All cost estimates are in 1992 dollars.
8. Propulsion costs are not eroded with a learning curve. They were considered a fixed cost from the airframer's perspective.
9. The effects of the structural concept and process alternatives on the maintenance of the aircraft were not considered. Hence, variations in DOC for the concepts are due only to differentials in financing, interest, depreciation, and insurance costs for the aircraft.

Cost versus Performance Studies

The first plots are normalized with respect to Concept 1. Figures 14-17 show a series of comparisons of product and process metrics for the wing, the aircraft, and the operating costs. These plots represent product *and* process trades that can be used to evaluate feasible alternative wing structural concepts, as related to Figures 2a and 2b.

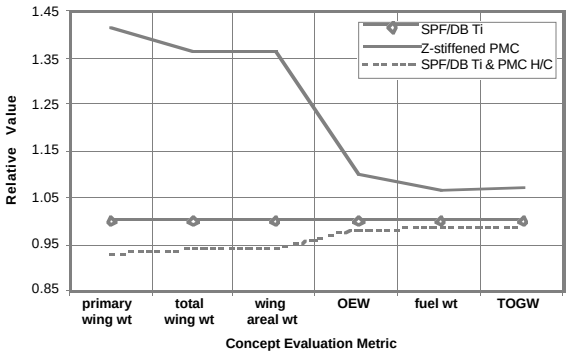

Figure 14 Component and System Weights

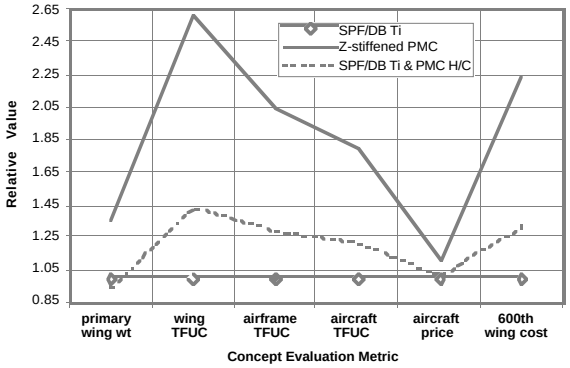

Figure 15 Component and System Costs

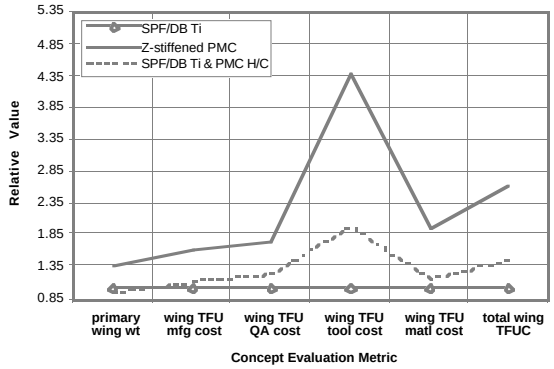

Figure 16 Sub-component and Component Costs

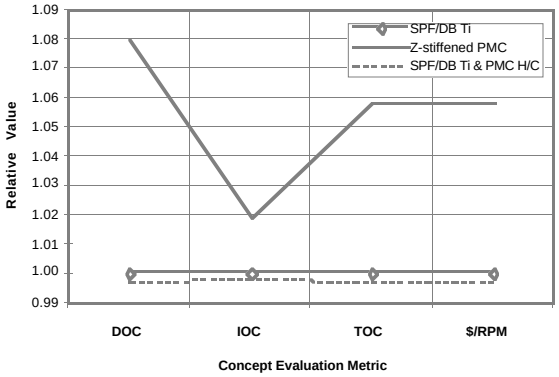

Figure 17 Operating Costs

Figure 14 shows several standard product evaluation metrics that are used to evaluate concepts during conceptual design. The three wing concepts show the intuitive trend: the concept with the lowest weight (concept 3) corresponded to the aircraft with the lightest OWE, least mission fuel required for the design range, and lightest TOGW. The heaviest wing concept (concept 2) resulted in the heaviest OWE, most mission fuel required, and heaviest aircraft TOGW. One might expect the composite wing concept to weigh less than the titanium concept. However, since much of the HSCT wing structure experiences light to heavy bi-directional loads, the discretely-stiffened PMC concept is much heavier due to its inability to resist the biaxial loads as well as the SPF/DB panels or the PMC honeycomb panels in concepts 1 and 3.

Figure 15 shows some interesting trends. The hybrid concept, which had the lowest wing weight, has a TFUC approximately 40% higher than the slightly heavier SPF/DB concept. The Z-stiffened PMC concept is substantially higher than both of the other concepts. The airframe and aircraft TFUCs exhibit the same trends, but with smaller relative magnitudes. However, when the various manufacturing costs, tooling costs, material costs, and learning curves are all considered simultaneously, the *prices* required for the manufacturer to make a 12% ROI on the production investment for 600 units are much closer in magnitude. The Z-stiffened PMC concept price is about 15% more than the SPF/DB concept. *The price for the hybrid concept was slightly higher than that of the SPF/DB concept, even though it weighed less.* A significant consequence of this will be noted later.

The TFUCs for the wing labor and materials are shown in Figure 16. The relative magnitude of the TFU tooling costs for the concepts is quantified in the figure. The TFU tooling costs for the heavy PMC Z-stiffened concept are extremely high, when compared to the other concepts.

The interesting effect of the differences in price between the all SPF/DB titanium wing concept and the hybrid concept are evident in Figure 17. Recall that the price of the lighter aircraft with the hybrid wing structure was higher than that of the aircraft with the all SPF/DB titanium structure. One might expect that, according to assumption (9), the operating costs for the hybrid aircraft would be more than that of the other. As shown in Figure 14, the mission fuel required by the aircraft with the hybrid wing was less than that for the aircraft with the all SPF/DB wing. *The higher price of the hybrid concept was more than offset by the lower fuel cost to fly the mission. Hence, the DOC of the*

aircraft with the hybrid wing structure is less than that of the aircraft with the all SPF/DB titanium wing. This type of result is precisely that which can be used for the economic justification of a major design decision. It illustrates the cost trade-off between production and O&S costs.

Cost/Time Analyses

The next set of plots are cost/time analysis plots (refer to Figure 5). Cost/time curves are plotted for the constituents of the total direct recurring labor (fabrication and assembly, quality assurance or inspection, and tooling). The sum of the three labor components yields the total labor curve, shown as the dotted line in Figures 18-20.

The plots show the costs for production quantities from the 10th unit to the 1000th unit. The farthest point on the lower right end of each curve is the 10th unit; the highest point on the left end of each curve represents the 1000th unit.

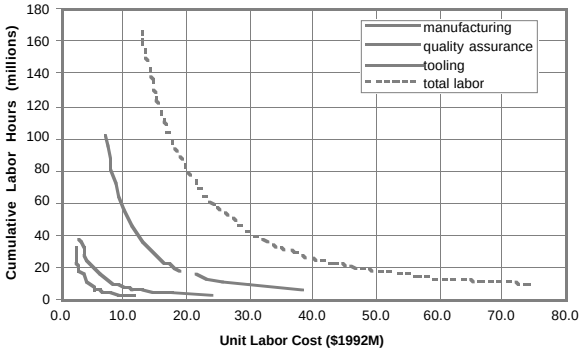

Figure 18 Concept 1 Labor Cost/Time Analysis

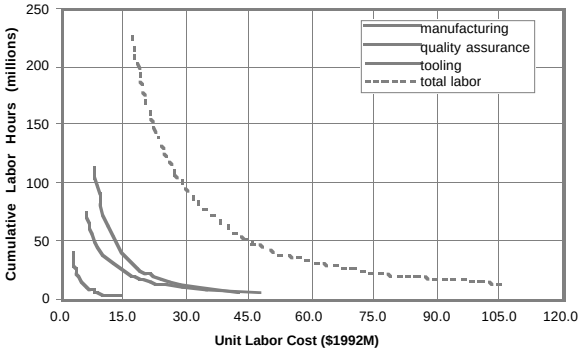

Figure 20 Concept 3 Labor Cost/Time Analysis

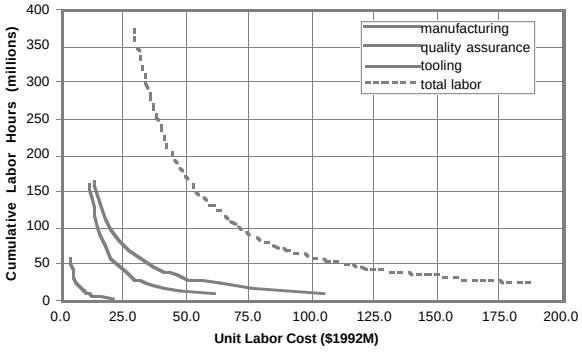

Figure 19 Concept 2 Labor Cost/Time Analysis

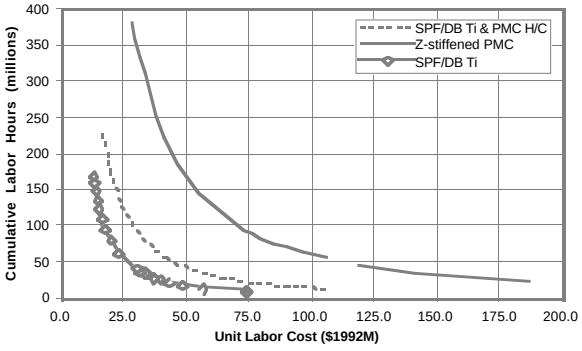

Figure 21 Labor Cost/Time Analysis: All Concepts

The use of the Cost/Time analyses can help identify the key cost drivers that are not evident when only considering the individual component manufacturing costs or cost of the entire aircraft. For all three concepts, the quality assurance costs, both in terms of dollars and hours, are the smallest cost element of the wing labor for any production quantity.

Close investigation of the tooling and manufacturing cost/time curves in the figures reveals several interesting trends. For concept 1, the all SPF/DB titanium concept plotted in Figure 18, the manufacturing (fabrication and assembly) cost and time are greater than the tooling cost and time for all production quantities.

As indicated previously in Figure 16, the TFUC of the tooling for the Z-stiffened PMC wing is much higher than that of the other two concepts. The high tooling cost (in terms of dollars) for low production quantities for this concept is evident in Figure 19. For the lower production quantities, the tooling cost is much greater than the manufacturing cost in dollars while being approximately equal in hours. As the production quantity increases, the dollar costs of the tooling decline to be nearly equal to the manufacturing dollar costs.

The hybrid baseline concept has the most interesting CTA plot, shown as Figure 20. For the lower production quantities, the tooling dollar costs exceed the manufacturing dollar costs with the hours being nearly equal. However, as the production quantity increases, the tooling costs fall below the manufacturing costs both in terms of dollars and hours.

The total labor cost/time curves are plotted in Figure 21 to show the relative total labor costs for the three wing concepts. Concept 2 has the highest labor cost for all production quantities while concept 1 has the lowest total labor cost for all production quantities.

As suggested by Resetar *et al*,[38] distinct learning curves were used for each component of the labor and material costs. This was implemented in ALCCA, and the results are clearly visible when plotted in log-log format in Figures 22 and 23. The figures present the wing costs and some of the aircraft major component costs for the hybrid wing concept relative to production quantity.

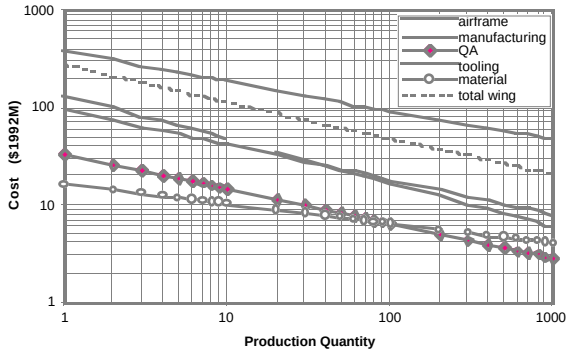

Figure 22 Concept 3 Wing and Airframe Costs

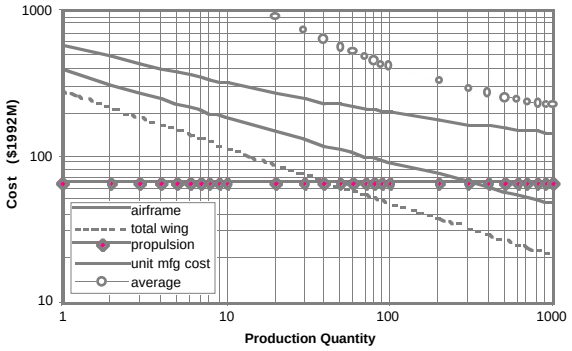

Figure 23 Concept 3 Component and System Costs

The effect of a learning curve is to reduce the production cost by a specific fraction each time the cumulative production doubles. When plotted in log-log format, the result is a straight line. The steeper the learning curve, the higher the initial costs, but the more the costs decrease as cumulative production increases. The tooling labor costs have the steepest slope in Figure 22.

The airframe and wing costs are shown again in Figure 23 for comparison to the total unit manufacturing cost and average unit cost (including all amortized RDT&E, production, and sustaining costs). The effect of assumption 8 (the fixed propulsion costs) is shown by the propulsion costs not changing as the production quantity increases. This results in the non-linear curve for the unit manufacturing costs.

Figures 24 and 25 show the annual and cumulative manufacturer cash flow distributions for HSCT production with the baseline wing structural concept.

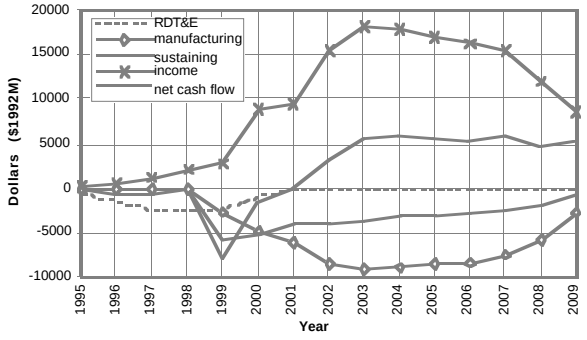

Figure 24 Concept 3 Annual Cash Flow

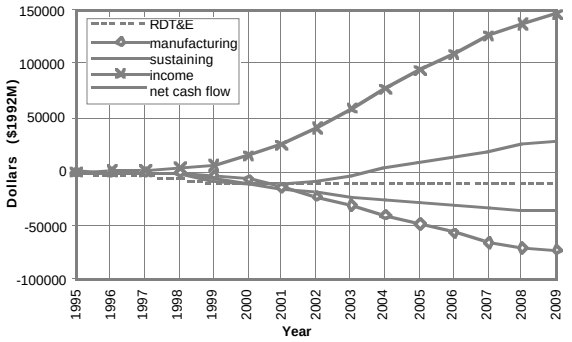

Figure 25 Concept 3 Cumulative Cash Flow

Figure 24 shows the annual cash flows over the assumed 60 month period of pre-production and the 10 year production period. RDT&E costs are distributed over the first 72 months of the program. The plot of the revenue clearly shows the order payments and delivery payments corresponding to the delivery schedule. The annual net cash flow is negative for the first six years of the program, but is positive for the remaining nine years of the program.

The cumulative annual cash flows are shown in Figure 25. The most interesting line on the plot is the cumulative net cash flow. For a 600 unit production

run, with the aircraft selling at a price that corresponds to a 12% ROI for the manufacturer, the break-even point is approximately nine and a half years into the production; and the break-even unit was 365.

While these plots are interesting, the comparisons of discounted ROI versus price show more of an effect that a designer or production manager may like to know. The cash flows must be calculated to determine the internal rate of return. Figure 26 shows a plot of manufacturer's internal rate of return versus the selling price of the aircraft for aircraft with the three wing concepts.

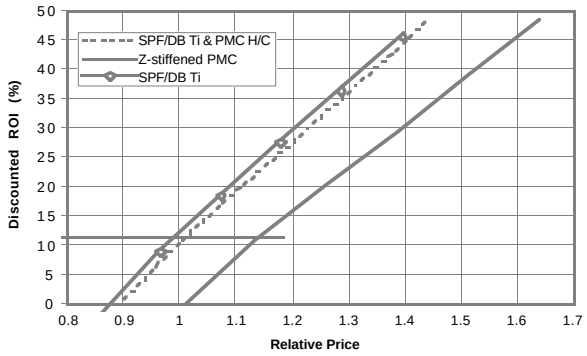

Figure 26 Manufacturer's ROI vs. Aircraft Price

The horizontal line in the figure is placed at 12% ROI for the manufacturer. As shown, the price of the aircraft with the hybrid wing concept is slightly higher than that of the aircraft with the all SPF/DB wing concept. The price for concept 2 is almost 10% higher than that of concept 1.

Conclusions

In terms of both the product and process trades, the Z-stiffened PMC wing concept is not a viable structural concept. Its inability to support the bi-directional load distribution resulted in it having the highest wing weight, OWE, TOGW, and mission fuel. Its large weight and relatively expensive production costs yield an aircraft with the highest selling price and operating cost of the three concepts

Comparing and contrasting the remaining two concepts is not as simple. While the hybrid wing concept weighed less than the all SPF/DB titanium wing, all components of its total wing production costs were somewhat higher. However, when all RDT&E, manufacturing, and sustaining costs are amortized over the production of the aircraft, the resulting cash flows result in relatively similar selling prices for the aircraft to achieve a pre-specified ROI for the manufacturer. Though the aircraft with the hybrid wing had a higher selling price, its lower weight and required mission fuel reduce its direct operating costs to be slightly lower than those of the aircraft with the all SPF/DB titanium wing. This is an excellent example of a Cost versus Performance trade study result showing the balance between acquisition (production) costs and operational costs.

In terms of the functionality of the approach and implementation, the system was able to accurately reproduce the published performance[18] and economic[19] (including manufacturer and air carrier) results for the SST studies conducted by the Lockheed-California Company in the 1970s. The values predicted for HSCT operating costs and required revenue are consistent with the limited published HSCT economics data.[23]

Future Work

The case study presented in this paper showed the Life Cycle Cost implications of alternative structural concepts for the wing of the HSCT. The remainder of the work required to complete this research project will be to conduct sensitivity analyses due to perturbations of particular process variables for the baseline concept. These will be process trades that show the effects of under- or over-predictions for the fabrication, assembly, and tooling costs; the effects of different values for the learning curves and buy-to-fly ratios; and the effects of raw material costs, production quantity, and possibly production breakpoints on Life Cycle Costs.

Acknowledgments

This research is being funded under a NASA Langley Graduate Student Researchers Program (GSRP) Fellowship (NGT-51101). NASA Langley direction is provided by S. M. Dollyhigh at Langley Research Center. Tom Galloway of NASA Ames provides additional consultation for Design for Affordability studies.

Alex Velicki and Keith McIver of McDonnell Douglas provided much help with characterizing the concept product and process characteristics, respectively.

References

1 Fisher, D. C., "Design and Analysis Aid for Evaluating Aircraft Structures," Proceedings of the 2nd International Conference on Industrial and Engineering Applications of Artificial Intelligence and Expert Systems, Vol. 1, Tullahoma, TN, June, 1989.

2 Messimer, S. L., and Henshaw, J., "Composites Design and Manufacturing Assistant," International Journal of Materials and Product Technology, Volume 9, Nos 1/2/3, 1994.

3 Zumsteg, J. R., Pecora, D., and Pecora, V. J., "A Prototype Expert System for the Design and

Analysis of Composite Material Structures," Proceedings of the ASME International Computers in Engineering Conference, Boston, MA, 1985.

4 Pecora, D., Zumsteg, J. R., and Crossman, F. W., "An Application of Expert Systems to Composite Structural Design and Analysis," Proceedings of the ASME Winter Annual Meeting, Miami, FL, 1985.

5 Rao, K. P., Viswanath, S., Sridhara Murthy, S., and Jayatheertha, C., "An Expert System Approach for the Design of Composite Laminates," Journal of the Indian Institute of Science, Vol. 70, 1990.

6 Warburton, L. M., and Glatfelter, J. W., "Development and Utilization of a Knowledge-Based Environment on a Production Helicopter Program," Proceedings of the AHS Vertical Lift Aircraft Design Conference, San Francisco, CA, January, 1995.

7 Williams, M. J. R., "Automated Aircraft Engine Development Cost Estimating Using Artificial Intelligence," Oral Paper presented at the 27th AIAA Joint Propulsion Conference, Sacramento, CA, 1991.

8 Mabson, G. E., Flynn, B. W., Ilcewicz, L. B., and Graesser, D. L., "The Use of COSTADE in Developing Composite Commercial Aircraft Fuselage Structures," AIAA-94-1492, Proceedings of the 35th AIAA/ASME/ASCE/AHS/ASC Structures, Structural Dynamics, and Materials Conference, Hilton Head, SC, April, 1994.

9 Metschan, S. L., Wilden, K. S., Sharpless, G. C., and Andelman, R. M., "Cost Model Relationships Between Textile Manufacturing Processes and Design Details for Transport Fuselage Elements," Proceedings of the Third NASA ACT Conference, Long Beach, CA, June, 1992.

10 Lee, P., "A Process Oriented Parametric Cost Model," AIAA-93-1029, Proceedings of the AIAA/AHS/ASEE Aerospace Design Conference, Irvine, CA, February, 1993.

11 King, N. E., "Heuristics as a Design Tool for Brilliant Eyes Cost Engineering," AIAA-92-1055, Proceedings of the AIAA/AHS/ASEE Aerospace Design Conference, Irvine, CA, February, 1992.

12 Apgar, H., "Design-to-Life-Cycle-Cost in Aerospace," AIAA-93-1181, Proceedings of the AIAA/AHS/ASEE Aerospace Design Conference, Irvine, CA, February, 1993.

13 Meisl, C. J., "The Future of Design Integrated Cost Modeling," AIAA-92-1056, Proceedings of the AIAA/AHS/ASEE Aerospace Design Conference, Irvine, CA, February, 1992.

14 Solverson, R. R., "Design to Cost with PRICE H," AIAA-93-1030, Proceedings of the AIAA/AHS/ASEE Aerospace Design Conference, Irvine, CA, February, 1993.

15 Proceedings of the Defense Manufacturing Council/Industry Affordability Task Force Workshop, National Center for Advanced Technologies, Washington, D. C., March, 1995.

16 Noble, J. S., and Tanchoco, J. M. A., "Design for Economics," Chapter 16, Concurrent Engineering: Automation, Tools, and Techniques, edited by Andrew Kusiak, John Wiley & Sons, Inc., 1993.

17 Noble, J. S., and Tanchoco, J. M. A., "Concurrent Design and Economic Justification in Developing a Product," International Journal of Production Research, Vol. 28, No. 7, pp. 1225-1238.

18 Jensen, R. N., and Mijares, R. D., "Mass Analysis," Section 15, Substantiating Data for Arrow-Wing Supersonic Cruise Aircraft Structural Design Concepts Evaluation, NASA-CR-132575-4, October, 1975.

19 Sakata, I. F., "Production Costs," Section 16, Substantiating Data for Arrow-Wing Supersonic Cruise Aircraft Structural Design Concepts Evaluation, NASA-CR-132575-4, October, 1975.

20 Sakata, I. F., "Concept Evaluation and Selection," Section 17, Substantiating Data for Arrow-Wing Supersonic Cruise Aircraft Structural Design Concepts Evaluation, NASA-CR-132575-4, October, 1975.

21 Sakata, I. F., and Davis, G. W., "Evaluation of Structural Design Concepts for an Arrow-Wing Supersonic Cruise Aircraft," NASA-CR-2667, May, 1977.

22 Wright, B. R., and Ross, R. L., "Technology Assessment Studies Applied to Supersonic Cruise Vehicles," NASA CR-145133, September, 1976.

23 "High Speed Civil Transport Study," NASA-CR-4233, Boeing Commercial Airplanes, 1989.

24 Brunner, M., and Velicki, A., "Study of Materials and Structures for High Speed Civil Transports," NASA-CR-191434, McDonnell Douglas Aerospace, September, 1993.

25 Röhl, P. J., "A Multilevel Decomposition Procedure for the Preliminary Wing Design of a High Speed Civil Transport Aircraft," Ph.D. Thesis, School of Aerospace Engineering, Georgia Institute of Technology, Atlanta, GA, June, 1995.

26 "Study of High Speed Civil Transports," NASA-CR-4235, Douglas Aircraft Company, 1989.

27 Bhatia, K. G., and Wertheimer, J., "Aeroelastic Challenges for a High Speed Civil Transport," AIAA-93-1478, *Proceedings of the 34th*

AIAA/ASME/ASCE/AHS/ASC Structures, Structural Dynamics, and Materials Conference, La Jolla, CA, April, 1993.

28 Tzong, G., Baker, M. Yalamanchili, K., and Giesing, J., "Aeroelastic Loads and Structural Optimization of a High Speed Civil Transport Model," AIAA-94-4378, *Proceedings of the 5th AIAA/NASA/USAF/ISSMO Symposium on Multidisciplinary Analysis and Optimization*, Panama City Beach, FL, September, 1994.

29 Markus, A., "Resin Transfer Molding for Advanced Composite Primary Wing and Fuselage Structures," *Proceedings of the 2nd NASA ACT Conference*, Lake Tahoe, NV, November, 1991.

30 Markus, A., Thrash, P., and Rohwer, K., "Progress in Manufacturing Large Primary Aircraft Structures Using the Stitching/RTM Process," *Proceedings of the Third NASA ACT Conference*, Long Beach, CA, June, 1992.

31 Hatakeyama, S. J., "Wing Structures Development for the HSCT," *Aerospace Engineering*, May, 1995.

32 Suarez, J., and Dastin. S., "Comparison of Resin Film Infusion, Resin Transfer Molding, and Consolidation of Textile Preforms for Primary Aircraft Structure," *Proceedings of the 2nd NASA ACT Conference*, Lake Tahoe, NV, November, 1991.

33 Giarratano, J. and Riley, G., *Expert Systems: Principles and Programming*, PWS Publishing Company, Boston, MA, 1994.

34 McCullers, L. A., "FLOPS: Flight Optimization System," Release 5.7, User's Guide, NASA Langley Research Center, Hampton, VA, December, 1994.

35 Bobick, J. C., Braun, R. L., and Denny, R. E., "Documentation of the Analysis of the Benefits and Costs of Aeronautical Research and Technology Models - Volume 1: Technical Report," NASA-CR-152278, July, 1979.

36 Marx, W. J., Schrage, D. P., and Mavris, D. N., "An Application of Artificial Intelligence for Computer-Aided Design and Manufacturing," *Proceedings of the International Conference on Computational Engineering Sciences*, Mauna Lani, HI, July, 1995.

37 Marx, W. J., Mavris, D. N., and Schrage, D. P., "A Hierarchical Aircraft Life Cycle Cost Analysis Model," AIAA-95-3861, *Proceedings of the 1st AIAA Aircraft Engineering, Technology, and Operations Congress*, Los Angeles, CA, September, 1995.

38 Resetar, S. A., Rogers, J. C., and Hess, R. W., "Advanced Airframe Structural Materials: A Primer and Cost Estimating Methodology," Project AIR FORCE Report R-4016-AF, RAND Corporation, 1991.

39 *Military Handbook: Design Guidance for Producibility*, MIL-HDBK-727, April, 1984.

40 Carlson, H. W., and Walkley, K. B., "Numerical Methods and a Computer Program for Subsonic and Supersonic Aerodynamic Design and Analysis of Wings With Attainable Thrust Considerations," NASA-CR-3808, 1984.

41 McCullers, L. A., "AWAVE: User's Guide for the Revised Wave Drag Analysis Program," NASA Langley Research Center, Hampton, VA, September, 1992.

42 Harris, R. V., Jr., "An Analysis and Correlation of Aircraft Wave Drag," NASA TMX-947, March, 1964.

43 Middleton, W. D., and Lundry, J. L., "A System for Aerodynamic Design and Analysis of Supersonic Aircraft," *Part 1 - General Description and Theoretical Development*, NASA CR-3351, 1980.

44 Middleton, W. D., Lundry, J. L., and Coleman, R. G., "A System for Aerodynamic Design and Analysis of Supersonic Aircraft," *Part 2 - User's Manual*, NASA CR-3352, 1980.

45 Middleton, W. D., Lundry, J. L., and Coleman, R. G., "A System for Aerodynamic Design and Analysis of Supersonic Aircraft," *Part 3 - Computer Program Description*, NASA CR-3353, 1980.

46 Middleton, W. D., and Lundry, J. L., "A System for Aerodynamic Design and Analysis of Supersonic Aircraft," *Part 4 - Test Cases*, NASA CR-3354, 1980.

47 Velicki, A. "Materials and Structures for the HSCT," *Aerospace Engineering*, April, 1995.

48 Phone conversations with K. McIver, McDonnell Douglas Aerospace, Long Beach, CA, January, 1996.